Measurement of Strain Due to Bending and Axial Loads

Student Name
With
Partner Names

Report No. ASE369K-BAS2

ASE/EM Department
The University of Texas at Austin
Austin, TX 78712

December 3, 2004

Measurement of Strain Due to Bending and Axial Loads

Aluminum specimens were statically loaded for analysis in the Measurements Laboratory of W. R. Woolrich Laboratories at the University of Texas at Austin. A cantilever beam was loaded at the tip, and data was recorded from base-mounted strain gages. Several strain calculations were made using strain gage resistance changes, Wheatstone bridge circuits, and a Vishay strain gage conditioner and amplifier system. The values for strain for the varying methods were comparable to theoretical strain in a cantilever beam, especially the Wheatstone half-bridge circuit measurements. A tension specimen was loaded in to an Instron load cell for axial stress analysis. Stess-strain plots were calculated based on strain gage output, extensometer deflection measurements, and the constant cross-head speed of the load cell. Calculated strains were comparable to theoretical data, except for the strain based on the constant cross-head speed. Deflection in the end sections of the aluminum specimen as well as flexing in the load cell itself led to calculated strains that were three times higher than the theoretical strain based on a Young's modulus of 10 million psi. This experiment allowed for valuable experience with electrical resistance strain gages and methods by which to take strain gage data.

Table of Contents

1 Introduction

In engineering design, it is very often necessary to test hardware for stress and strain capabilities. For example, the Boeing 777 was subjected to full-size static testing to gain knowledge of the stress and strain potentials of the aircraft. The 777 was fitted with approximately 1500 electrical strain gages to monitor the loads on the vehicle during the free floating body test [1]. Accurate measurement of strain is crucial in the design and testing phase of nearly all aerospace vehicles.

This lab focuses on the measurement of stress and strain through the use of strain gages like those used in the testing of the 777. Through the use of hand constructed Wheatstone bridge circuits and a Micro-Measurements Strain Gage Conditioner and Amplifier System, base strain for a tip-loaded cantilever will be measured. The results for the differing measurement approaches will be compared with each-other as well as with theoretical values. A tensile specimen will be axially loaded in an Instron load cell. Strain calculations based on strain gage output, extensometer data, and the constant load cell cross-head speed will be compared in a stress-strain plot. A brief error analysis will be performed to help justify discrepancies between various forms of measurement and theoretical data.

2 Theory

2.1 Strain Gages

In this experiment, the strain gages utilized were foil-type electrical resistance strain gages. These gages are based on the principle that wire resistances change when the wires are subjected to mechanical strain [2]. An pair of electrical resistance strain gages can be seen in Figure 1.
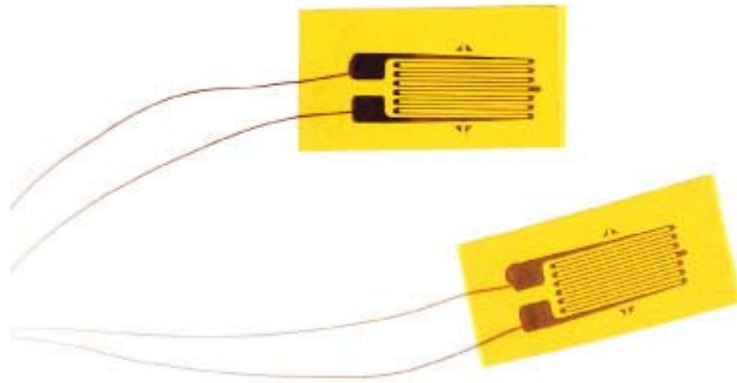
Figure 1: Electrical Resistance Foil Strain Gages [3]

These gages are bonded to the surface of the specimen to be measured. As the specimen elongates or deforms, the wires in the strain gage also elongate. This in turn causes a change in resistance and thus a change in voltage over the gage. The change in resistance is directly related to the strain by means of the gage factor, G [4].

$$\varepsilon = \frac{\Delta R / R}{G}$$

Therefore, a given resistance variance indicates the strain on the surface to which the gage is bonded.

2.2 Wheatstone Bridge Circuits

The resistive Wheatstone bridge circuit is frequently used in measurement systems. A bridge circuit can be seen in Figure 2. The boxes 1-4 are either resistors or resistive transducers, depending on the bridge setup. In this lab, the active resistive transducers are the electrical resistance strain gages. For a quarter-bridge, box 1 is an active strain gage, and all other boxes are fixed resistance resistors. In a half-bridge, boxes 1 and 2 are strain gages, and the others are resistors [5].

Figure 2: Wheatstone Bridge with Balance Potentiometer [4]

By applying Kirchhoff's current and voltage laws, the output of the Wheatstone bridge circuit pictured in Figure 2 is given by
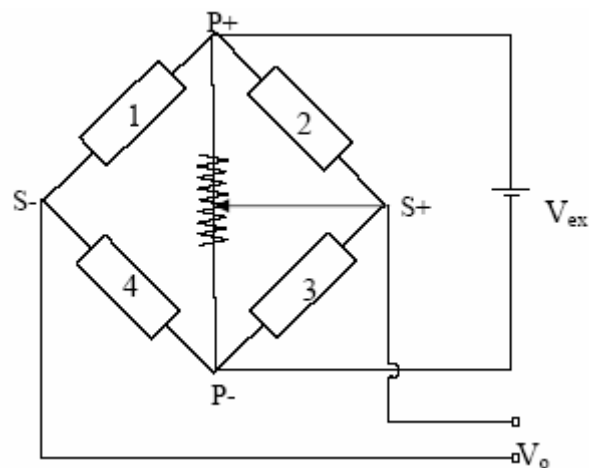
$$V_o = \frac{V_{ex}}{4}\left(\frac{\Delta R_1}{R_1} - \frac{\Delta R_2}{R_2} + \frac{\Delta R_3}{R_3} - \frac{\Delta R_4}{R_4}\right).$$

So, for a quarter bridge

$$V_o = \frac{V_{ex}\Delta R_1}{4R_1},$$

and for a half bridge

$$V_o = \frac{V_{ex}}{4}\left(\frac{\Delta R_1}{R_1} - \frac{\Delta R_2}{R_2}\right).$$

For a strain gage,

$$\frac{dR}{R} = \left(\frac{1}{L}\frac{\partial L}{\partial \varepsilon} - \frac{1}{A}\frac{\partial A}{\partial \varepsilon}\right)\partial\varepsilon = \frac{dL}{L}(1+2\upsilon) = G\varepsilon$$

where L is the specimen length, A is the specimen cross sectional area, ε is the strain, and G is the gage factor [4]. Substituting in to the quarter and half-bridge equations for V_o,

$V_o = V_{ex}G\varepsilon_1/4$ and $V_o = \frac{V_{ex}G}{4}(\varepsilon_1 - \varepsilon_2)$ respectively. Therefore, the voltage output for a

quarter bridge is directly proportional to the strain that the gage is measuring. The half-bridge voltage output is proportional to the difference in strains between the two gages.

2.3 Calibration Resistance

It is possible to find the sensitivity of a Wheatstone bridge configuration by shunting a gage of the arrangement with a known resistance. This procedure can be seen in Figure 3 where the known resistance is R_s. The simulated strain over R_2 can be found using the equation [4]

$$\varepsilon_2 = \frac{\Delta R_2}{GR_2}, \text{ where } \Delta R_2 = -\frac{R_2^2}{R_2 + R_s}.$$

The sensitivity for the gage can then be determined by dividing the shunted output voltage by the strain ε_2.

$$S_{\varepsilon_2} = \left|\frac{V_o}{\varepsilon_2}\right|$$

In this experiment, the Vishay amplifier system has calibration switches that place an equivalent strain of $\pm1000\mu\varepsilon$ on the bridge circuit, from which the sensitivity of the circuit can then be determined. Strains can then be calculated by solving the above equation for ε. In the case of a half-bridge, it is necessary to account for both stains by plugging in $\varepsilon_1 - \varepsilon_2$ so that

$$S_\varepsilon = \left| \frac{V_o}{\varepsilon_1 - \varepsilon_2} \right|.$$

Again, calibration resistances allow for a sensitivity to be established so that output voltages can easily and accurately be converted into strain.
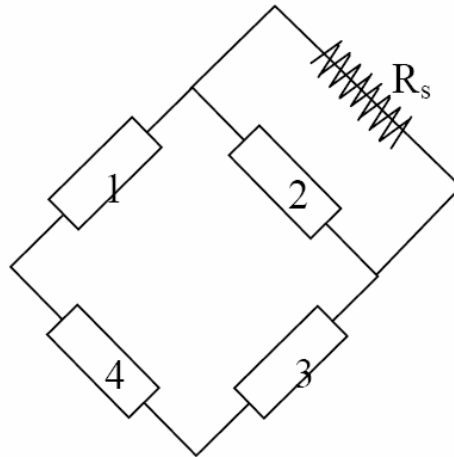
Figure 3: Wheatstone Bridge with Shunt Resistor R_s [4]

2.4 Cantilever Beam Bending

When subjected to a point load at its tip, a cantilever beam has a linear variance in stress and strain through the cross-section in the direction parallel to the load. The stress and strain at the center of the beam is zero. Therefore, the strain on the top and bottom of the beam are equal, opposite, and maximum. So for the setup in Figure 4, strain gage G1 should read an equal and opposite strain to that of G2. To calculate the stress [6],

$$\sigma = \frac{My}{I}.$$

I is the moment of inertia and for a rectangular cross section, $I = bh^3/12$ where b is the base and

h is the height [6]. At the base of the beam, the moment is $M = WL$.
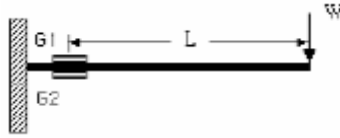
Figure 4: Cantilever Beam with Tip Load [4]

At the surface, $y = h/2$. Plugging in to the stress equation, the stress on the surface at the base of

the beam is

$$\sigma = \frac{6WL}{bh^2}.$$

Strain can then be directly calculated using Hooke's Law, $\varepsilon = \sigma/E$ [6] when assuming a

maximum Poisson's ratio of 0.5. To maximize the sensitivity when measuring strain, a half-

bridge circuit is utilized with strain gages in positions 1 and 2 of Figure 2. Because the bottom

gage will have a negative strain opposite to that of gage 1, the output voltage will be

approximately twice the voltage that would be seen in a quarter-bridge circuit. The surface strain

and tension can then be found by dividing the output voltage in half.

2.5 Axial Tension

A uniform rod in axial tension has equal strain through a given cross section. Figure 5

depicts a tension specimen in axial tension similar to the bar analyzed in this experiment. The

thinner section of the bar is the gage section. The larger cross-sectional ends are for mounting

purposes. The deflection of the bar can be used to calculate the strain by means of the equation

$$\varepsilon = \frac{\delta}{L}$$

where δ is the deflection and L is the length of the bar [6]. Stress in an axial member is

$$\sigma = \frac{P}{A}$$

where P is the force imparted on the bar and A is the cross-sectional area of the gage section [6]. A Wheatstone half-bridge with gages G1 and G2 on opposing sides of the bar at positions 1 and 2 of the Wheatstone bridge of Figure 2 would therefore result in an output voltage of nearly zero. To gain valuable data, a quarter-bridge or a half-bridge with the gages at positions 1 and 3 must be used. The half-bridge is more sensitive, as was the case for the cantilever.
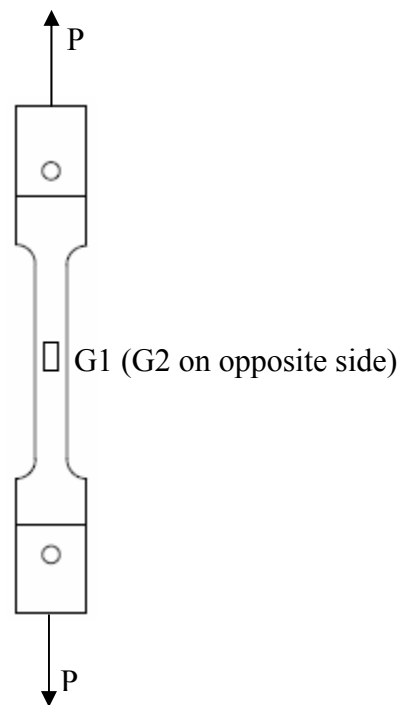
Figure 5: Bar in Axial Tension [4]

2.6 Accounting for Temperature Effects

Changes in temperature affect strain output. One way to eliminate these effects for the cantilever beam under a tip load is by utilizing the half-bridge. The temperature effects will be equal on the gages on each side of the beam, and will therefore cancel out. The output voltage will be independent of temperature. To eliminate the temperature effects in axial loading, it is best to construct a full-bridge with dummy gages at positions 2 and 4 of Figure 2 and the elongating gages at 1 and 3. The dummy gages will respond to temperature changes with equal resistance differences to the variations experienced by the gages on the tension specimen. They will therefore cancel out, and the output voltage will be independent of temperature [7].

2.7 Quantitative Error Analysis

An uncertainty calculation is necessary to quantitatively examine the errors associated with measured values throughout the experiment. Uncertainty in measurements propagates to uncertainties in calculated values. Assume we have a function f(x,y), known measured values of x and y, μ_x and μ_y, and their uncertainties σ_x and σ_y. The expected value and variance of f is expressed by

$$\mu_f = f(\mu_x, \mu_y) \text{ and } \sigma_f = \sqrt{\left(\frac{\partial f}{\partial x}\sigma_x\right)^2 + \left(\frac{\partial f}{\partial y}\sigma_y\right)^2}.$$

Therefore, the calculated quantity f(x,y) can be off by as much as σ_f / μ_f based on the uncertainty in measured quantities x and y [8].

3 Apparatus and Procedures

3.1 Apparatus

Several pieces of equipment were utilized in the strain analysis. A Protek 3015B DC power supply provided power to the Wheatstone bridge circuit. A balance unit was used to set up and balance the bridge circuits. A Dell Optiplex GX260 PC, serial # 00045-162-170-499 was utilized to run National Instruments DAQ and VirtualBench. The Instron Model 3367 load frame and load cell, serial # 3367P8675 provided the tensile stress and a form of strain measurement. An aluminum cantilever beam was used to measure tensile and compressive stress caused by a tip load. Another aluminum specimen was analyzed under tension in the Instron load frame. Each aluminum specimen had 2 strain gages bonded on opposing sides. The gage factors were 2.11 and 2.05 for the cantilever beam and tension specimen, respectively.

3.2 Procedures

Several methods of strain measurement were performed for a cantilever beam subjected to a tip load and a beam under axial tension. Before beginning the experiment, we closely examined the strain gages and leads to make sure that the gages were well bonded to the beams. Our aluminum specimens had well connected strain gages, so we were ready to perform the experiment.

3.2.1 The Wheatstone Bridge and its Application in Strain Measurement

The aluminum beam was mounted tightly in the angle bracket on the load frame, in a similar manner as seen in Figure 4. Before beginning to take strain measurements, it was

necessary to measure all dimensions of the specimen so that the theoretical strain can be calculated. The aluminum beam dimensions were measured using a ruler and a micrometer. The weight applied to the tip of the beam was given to be 2.176 lb.

To measure the strain in the beam with maximum sensitivity when it is loaded, a half-bridge Wheatstone circuit will be utilized. Before the circuit was created, the strain gage resistances were measured with no weight on the beam. The weight was then applied and the resistances were again measured.
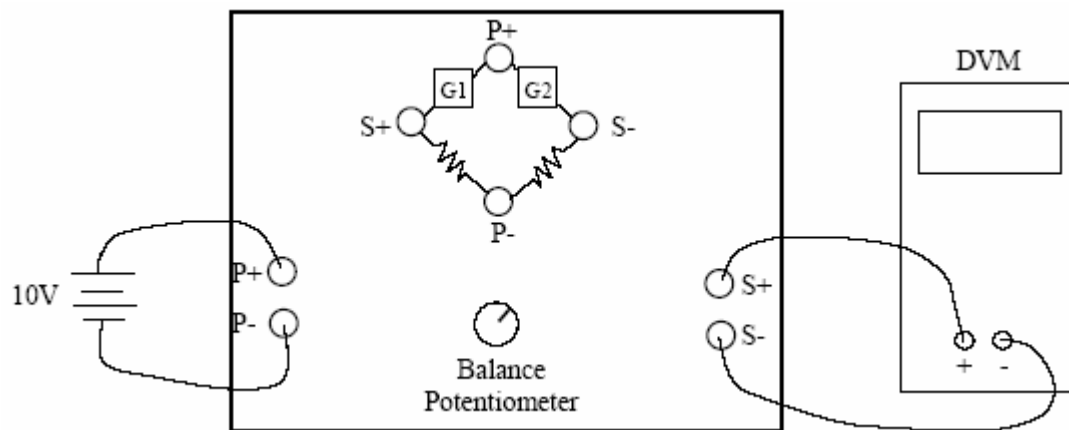
Figure 6: Balance Unit Input/Output Setup [4]

Using the balance unit, the power supply, and the digital volt meter (DVM), a half-bridge was constructed as seen in Figure 6. Two 120 Ω resistors were used to complete the Wheatstone bridge. Before connecting the power, the circuit input resistance and output resistance were measured. The input voltage was set to 10 V and the output voltage was zeroed out by adjusting the balance potentiometer. After being zeroed, the output voltage proceeded to drift off of zero, to a positive voltage of 0.065 mV. To gain a feel for how the circuit reacts to inputs, a student deflected the tip of the beam downward approximately one inch. The corresponding output

10

voltage was -8.6 mV. When deflecting the beam upward, the output was approximately 8.9 mV.

In both cases, the output voltage did not return precisely to the initial offset of 0.065 mV. With

the 2.176 lb weight placed on the tip of the beam, the output read -9.56 mV. After removing the

weight, the output returned to 0.043 mV.

A quarter-bridge circuit was then created by replacing the lower gage G2 from the circuit

with a 120 Ω resistor. The weight was applied to the end of the beam and the output voltage was

measured. After removing the weight, a group member warmed the strain gage by holding their

hand on the gage to see the effects of temperature on strain gage performance. The output

voltage was -0.291 mV. The power supply was then turned off and the bridge circuit was

unwired in preparation for the next portion of the experiment.

3.2.2 Vishay Micro-Measurements Strain Gage Conditioner and Amplifier System

The wiring diagrams and instructions for the Vishay equipment were found in the

instruction manual. The METER output of the amplifier box was connected to the DVM and the

excitation voltage was brought to approximately 2 V by adjusting the screw in the first panel.

The top strain gage was connected to the amplifier using the 8-terminal amplifier cable as

specified in the instruction manual for a quarter-bridge circuit. The DVM was again set up to

measure the amplifier output. The amplifier was then powered up and the bridge was balanced

using the balancing potentiometer to a voltage of -0.10 mV. To allow for gage calibration, the

calibration switch was moved to position A, and the output voltage was recorded. The voltage

was measured when the calibration switch was in position B as well. The calibration switch was

then returned to the middle position.

After zeroing and calibrating the bridge circuit, the 2.176 lb weight was applied to the end of the beam and the output voltage was measured using the DVM.   This voltage will be converted to strain and compared to the strain calculated from the Wheatstone bridge circuit that the group constructed. After completing the quarter-bridge measurements, both strain gages were connected to the amplifier according to the half-bridge circuit diagram in the instruction manual. The circuit was balanced to -0.09 mV, and the calibration voltages were again measured. The weight was hung from the beam and the output voltage was recorded. The amplifier was then turned off and the circuitry was disassembled.

3.2.3 Measurement of the Elastic Stress-Strain Curve in a Tensile Specimen

Before subjecting the aluminum specimen to the tensile test, the gage cross-section was measured. The bar was then mounted in the Instron loading frame. One of the strain gages on the bar was connected in a quarter-bridge configuration to the amplifier. The bridge was balanced and calibrated in a similar manner to that which was utilized in the previous section. The Series IX software for the load frame was launched on the Dell PC. The load cell was balanced by zeroing the load in the software. The clip-gage extensometer was calibrated, connected to the specimen at the same location as the strain gage, and then balanced. The VirtualBench Logger was opened to record the data from the strain gage amplifier. The dimensions of the bar were input to the Series IX program and the tensile test was run up to a 1000 lb load. The outputs of both the strain gage and the extensometer were saved off to text files for stress and strain analysis.

After data files were saved off, the teaching assistant manually returned the cross-head to its starting position. The aluminum tension specimen was removed from the loading frame and all circuitry was disconnected. Data files were emailed to class members for analysis.

4 Results

4.1 Cantilever Beam Strain Analysis

Several different methods for determining the surface strain at the base of a cantilever beam were utilized in this experiment. The measured dimensions for the cantilever beam are shown in Table 1. The length was measured from the mounted edge to the point at which the weight was hung. These dimensions were used to calculate a theoretical strain at the base of the beam.

Table 1: Cantilever Beam Dimensions (in.)

Length	10.77
Width	0.9844
Thickness	0.126

With a tip load of 2.176 lb, the stress at the base was calculated to be 8993 psi. The microstrain is then calculated by dividing by Young's modulus and multiplying by 10^6. For aluminum, $E \approx$ 10e6 psi. This results in a microstrain of 899. After measuring the strain gage resistances with and without the weight on the beam, the microstrain for the gages was calculated using $\varepsilon = \Delta R/R\,G$. The results can be seen in Table 2.

Table 2: Microstrain Calculation Using Gage Resistances

	Strain Gage Resistances (Ω)		microstrain
	Without Weight	With Weight	
G1	120.46	120.64	708
G2	120.75	120.49	1020

The Wheatstone half-bridge was constructed by hand as another means to calculate the strain at the base of the beam. After balancing the unloaded circuit, the input resistance was measured to be 119.42 Ω and the output resistance was 119.70 Ω. As expected, these are similar to the gage resistances measured before the circuit was assembled. Applying the weight resulted in a negative voltage of 9.56 mV. Plugging in to the voltage-strain relation equation for a half-bridge from Section 2.2 and assuming that the two strains are equal and opposite, the base microstrain is calculated to be 906. The quarter-bridge configuration resulted in an output voltage of -4.82 mV. This voltage corresponds to a microstrain of 914 for a quarter-bridge.

A final mode for calculating the strain at the base of the beam was with the Vishay equipment. A quarter-bridge circuit was assembled and the sensitivity of the gages was calculated using the method outlined in Section 2.3. To more accurately calculate the sensitivity of the gages, the calibration voltages were offset by the near zero initial voltage, and then averaged. The 2.176 lb weight was applied to the end of the beam and the output voltage was measured to be 15.01 mV. When the same procedure was executed for the half bridge, the output voltage was 3.760 mV. These voltages along with the average calibration voltages were used to calculate the microstrain of the beam base. The sensitivity calculations are in Table 3 and the microstrains are in Table 4.

Table 3: Vishay Calculated Bridge Circuit Sensitivities

				Offset Values			
	Offset (mV)	CAL A (mV)	CAL B (mV)	CAL A (mV)	CAL B (mV)	Avg. CAL	S_ε (V/ε)
Quarter-Bridge	-0.1	16.15	-16.32	16.25	-16.22	16.235	16.235
Half-Bridge	-0.09	1.91	-2.11	2	-2.02	2.01	2.01

Table 4: Vishay Calculated Strains for Cantilever

	S_ε (V/ε)	V_o (mv)	ε_{tot}	ε	$\mu\varepsilon$
Quarter-Bridge	16.235	15.01	9.25E-04	9.25E-04	925
Half-Bridge	2.01	3.76	1.87E-03	9.35E-04	935

The total strain in Table 4 calculated from the sensitivity equations in Section 2.3 must be divided by 2 in the half-bridge configuration, since the gages have equal and opposite strains. A compilation of microstrain calculations is in Table 5.

Table 5: Microstrain Calculations Summary

	Microstrain	Uncertainty (%)
Theoretical	899	2.25
Gage Resistance (avg)	864	6.67
Self-Constructed Quarter-bridge	914	1.16
Self-Constructed Half-bridge	906	1.11
Vishay Quarter-Bridge	925	0.09
Vishay Half-Bridge	935	0.56

Uncertainty was calculated for all values of microstrain using the method outlined in Section 2.7. The measured error assumptions can be seen in Appendix A. The gage resistance based microstrain was accompanied by the largest error while the Vishay measurements had the lowest. The quarter-bridge uncertainty should be higher for both the constructed Wheatstone and Vishay measurements. It is possible that an inaccurate approximation for the calibration resistance averages was made in computing the uncertainty for the Vishay measurements. In any case, the uncertainties were low, and the calculated microstrain values did not vary more than 4% from the theoretical value.

4.2 Elastic Stress-Strain Curve for a Tensile Specimen

The elastic stress-strain curve of the aluminum tensile specimen was measured and calculated in several different ways. In order to calculate the theoretical stress, the cross sectional area was necessary. The specimen was 0.504 inches wide and 0.181 inches thick. From this, stress as a function of tensile force was calculated. Theoretical strain was then calculated assuming $E \approx$ 10e6 psi. Because the load cell displaces the top of the specimen at a constant 0.05 in/min, a displacement as a function of time can be calculated and used to compute strain. Stress can again be calculated by dividing force by cross-sectional area.

Stress as a function of time was calculated using two different methods based on the strain gage data in the quarter-bridge setup. The first used Wheatstone bridge relations from Section 2.2. The second used the calibration method outlined in Section 2.3. The zero-offset was -0.052 mV and the calibration voltages were 5.94 and -6.01 mV. As was done for the cantilever, the calibration voltages were offset and averaged to get a sensitivity in V/ε. In both strain gage calculations, it was necessary to determine force as a function of time from the load cell output so that stresses could be calculated. A fifth and final measurement of stress versus strain was based on extensometer data. Strain was calculated using $\varepsilon = \delta/L$ and stress was again calculated using $\sigma = P/A$.

All five stress-strain plots can be seen in Figure 7. Error bars were added to both sets of data pertaining to the strain gage. Uncertainties in stress were negligible, as were uncertainties in extensometer and load cell outputs. The assumed uncertainties in measured values can be seen in Appendix B. The constant cross-head speed had strains that were 3 times larger for a given stress than the theoretical data. The strain was calculated as a function of the elongation of the entire setup. The load-cell itself flexes under the load, and the end sections of the specimen

17

also elongate. Therefore, according to the data, the elongation of the gage section is only about one third of the elongation of the entire stack.

Figure 7: Stress vs. Strain
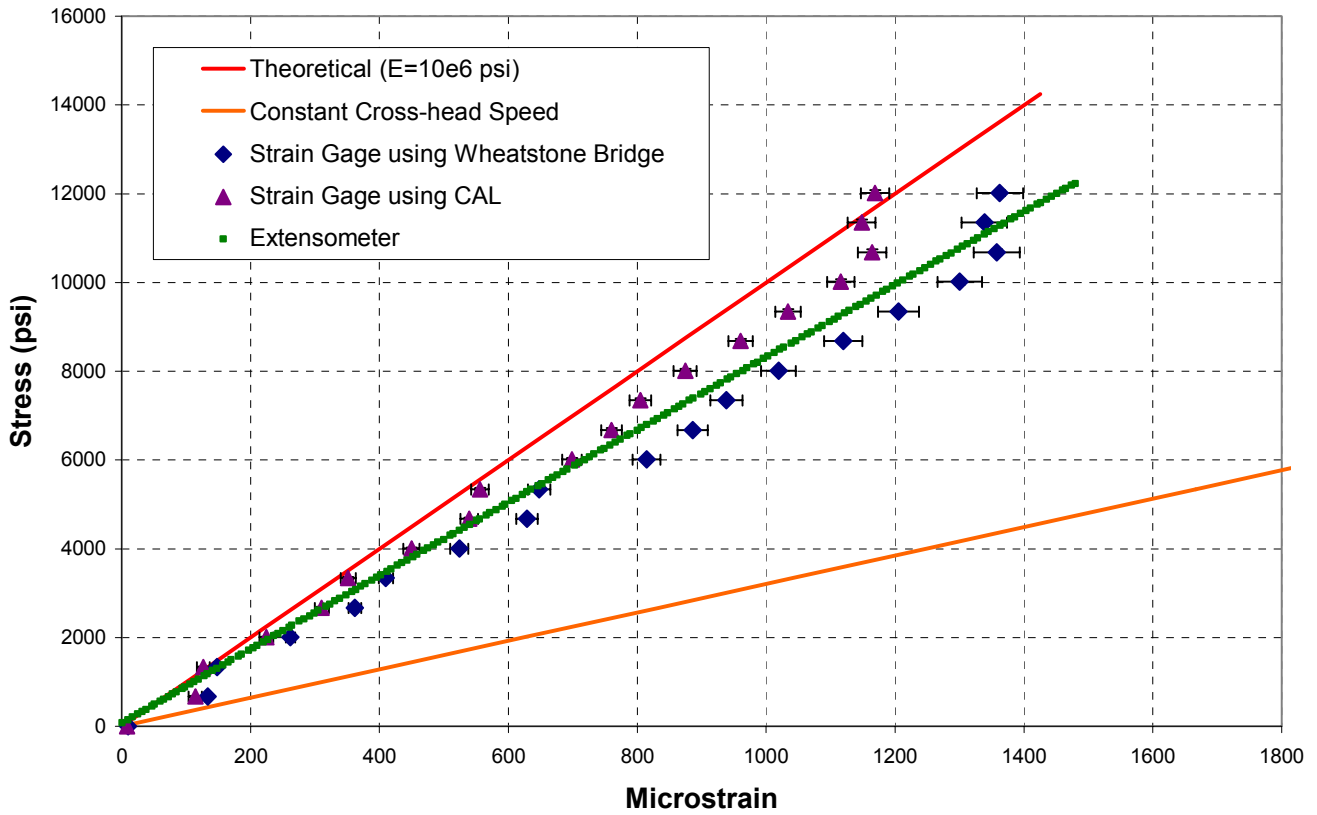
5 Conclusions

The generation of stress and strain values through several different modes of measurement allowed for an understanding of different measuring tools, and the errors associated with each. The calculation of base strain for a cantilever beam with a tip load was done with five different methods. Each agreed well with theoretical data, with the most accurate measurements occurring through the use of a Wheatstone bridge circuit. An aluminum specimen in tension was also analyzed. Strains based on constant load cell cross-head speed, strain gage data, and extensometer data were compared with theoretical strain on a stress-strain plot. The strain gage and extensometer derived strains were somewhat agreeable with theory, but the strains were much larger when assuming a constant elongation rate from the cross-head speed. The load cell apparatus flexed as the load increased, and the sections of the specimen outside of the gage section also elongated. For a given stress based on the load output of the load cell, the gage section did not elongate the full elongation of the load cell. Therefore, when assuming the elongation based on the cross-head speed, the strains were much higher.

6 References

1.	Schuster, S. A., "Testing the Structural Integrity of the Boeing 777," Sensors Magazine, URL: http://www.sensorsmag.com/articles/0296/777/ [cited 1 December 2004].

2.	Beckwith, T. G., Marangoni, R. D., and Lienhard, J. H., *Mechanical Measurements*, 5th ed., Pearson Education, 482 F.I.E. Patparganj, Delhi 110 092, India, p. 483.

3.	"The Strain Gage," URL: http://www.omega.com/literature/transactions/volume3/strain.html [cited 28 November 2004]

4.	Ravi-Chandar, K., "Lab #8: Measurement of Strain," pp. 2-3, 8-9, URL: http://www.ae.utexas.edu/courses/ase369k/labs/lab8_procedure.pdf [cited 20 November 2004].

5.	Stahl, B. A., "The Wheatstone Bridge," *Class Notes*, October 8, 2004.

6.	Gere, J. M., *Mechanics of Materials*, 5th Ed., Brooks/Cole, Pacific Grove, CA, 2001, pp. 4, 6, 324, 517.

7.	"Strain Gauge Configuration Types," *NI Developer Zone*, URL: http://zone.ni.com/devzone/conceptd.nsf/webmain/C18F65CE920C115086256D720058325B [cited 28 November 2004].

8.	Ravi-Chandar, K., "Probability and Statistics for Analysis of Experimental Data," p. 5, URL: http://www.ae.utexas.edu/courses/ase369k/pdf/Statistics.pdf [cited 15 October 2004].

Appendix A: Cantilever Beam Strain Uncertainty Estimates

Theoretical Strain Uncertainties

parameter	value	uncertainty		
W (lb)	2.176	0.001		
L (in)	10.7656	0.0156		
w (in)	0.9844	0.0156		
t (in)	0.126	0.001	$\Delta\varepsilon/\varepsilon =$	0.0225

Gage Resistance Strain Uncertainties

parameter	value	uncertainty		
Rweight (?)	120.64	0.01		
Rnoweight (?)	120.46	0.01	G1	
G	2.11	0.01	$\Delta\varepsilon/\varepsilon =$	0.0787
Rweight (?)	120.49	0.01		
Rnoweight (?)	120.75	0.01	G2	
G	2.11	0.01	$\Delta\varepsilon/\varepsilon =$	0.0547

Hand Constructed Wheatstone Strain Uncertainties

parameter	value	uncertainty		
Vo (mV)	9.56E-03	1.00E-05		
Vex (V)	10	0.1	half-bridge	
G	2.11	0.01	$\Delta\varepsilon/\varepsilon =$	0.0111
Vo (mV)	2.91E-04	1.00E-06		
Vex (V)	10	0.1	qtr-bridge	
G	2.11	0.01	$\Delta\varepsilon/\varepsilon =$	0.0116

Vishay Strain Uncertainties

parameter	value	uncertainty		
S (V/ε)	16.235	0.01	qtr-bridge	
Vo (V)	15.01	0.01	$\Delta\varepsilon/\varepsilon =$	0.0009
S (V/ε)	2.01	0.01	half-bridge	
Vo (V)	3.76	0.01	$\Delta\varepsilon/\varepsilon =$	0.0056

Appendix B: Tension Specimen Data

B.1 Theoretical Stress vs. Strain

Force (lb)	Stress (psi)	Strain	Microstrain
0	0	0.00E+00	0
100	1096	1.10E-04	110
200	2192	2.19E-04	219
300	3289	3.29E-04	329
400	4385	4.38E-04	438
500	5481	5.48E-04	548
600	6577	6.58E-04	658
700	7673	7.67E-04	767
800	8770	8.77E-04	877
900	9866	9.87E-04	987
1000	10962	1.10E-03	1096
1100	12058	1.21E-03	1206
1200	13154	1.32E-03	1315
1300	14251	1.43E-03	1425

B.2 Constant Cross-Head Displacement Stress vs. Strain

Time (s)	Displacement (in)	Force (lb)	microstrain	Stress (psi)	L (in) =	4
0	0.00E+00	0	0	0		
1	8.33E-04	60.9	208	668		
2	1.67E-03	121.8	417	1335		
3	2.50E-03	182.7	625	2003		
4	3.33E-03	243.6	833	2670		
5	4.17E-03	304.5	1042	3338		
6	5.00E-03	365.4	1250	4006		
7	5.83E-03	426.3	1458	4673		
8	6.67E-03	487.2	1667	5341		
9	7.50E-03	548.1	1875	6008		
10	8.33E-03	609	2083	6676		
11	9.17E-03	669.9	2292	7343		
12	1.00E-02	730.8	2500	8011		
13	1.08E-02	791.7	2708	8679		
14	1.17E-02	852.6	2917	9346		
15	1.25E-02	913.5	3125	10014		
16	1.33E-02	974.4	3333	10681		
17	1.42E-02	1035.3	3542	11349		
18	1.50E-02	1096.2	3750	12017		
19	1.58E-02	1157.1	3958	12684		
20	1.67E-02	1218	4167	13352		

B.3 Strain Gage Stress vs. Strain using Bridge Voltage Relations with Uncertainties

Time (s)	Ch0(V)	Ch0(mV)	Strain	microstrain	Force (lb)	Stress (psi)	Stress Uncertainty (psi)	Strain Uncertainty
0	4.88E-05	0.05	9.53E-06	10	0	0	0.00	0.00
1	6.84E-04	0.68	1.33E-04	133	60.9	668	11.64	4.02
2	7.57E-04	0.76	1.48E-04	148	121.8	1335	13.48	4.35
3	1.34E-03	1.34	2.62E-04	262	182.7	2003	16.07	7.18
4	1.86E-03	1.86	3.62E-04	362	243.6	2670	19.13	9.74
5	2.10E-03	2.10	4.10E-04	410	304.5	3338	22.45	10.97
6	2.69E-03	2.69	5.24E-04	524	365.4	4006	25.94	13.95
7	3.22E-03	3.22	6.29E-04	629	426.3	4673	29.54	16.69
8	3.32E-03	3.32	6.48E-04	648	487.2	5341	33.21	17.19
9	4.17E-03	4.17	8.15E-04	815	548.1	6008	36.93	21.56
10	4.54E-03	4.54	8.86E-04	886	609	6676	40.69	23.44
11	4.81E-03	4.81	9.38E-04	938	669.9	7343	44.48	24.82
12	5.22E-03	5.22	1.02E-03	1019	730.8	8011	48.29	26.94
13	5.74E-03	5.74	1.12E-03	1119	791.7	8679	52.11	29.57
14	6.18E-03	6.18	1.21E-03	1205	852.6	9346	55.95	31.83
15	6.67E-03	6.67	1.30E-03	1300	913.5	10014	59.80	34.34
16	6.96E-03	6.96	1.36E-03	1358	974.4	10681	63.65	35.84
17	6.86E-03	6.86	1.34E-03	1339	1035.3	11349	67.52	35.34
18	6.98E-03	6.98	1.36E-03	1362	1096.2	12017	71.39	35.97

B.4 Strain Gage Stress vs. Strain using Calibration Resistances with Uncertainties

S_ε (V/ε)	V_o (mV)	strain	microstrain	Force (lb)	Stress (psi)	Stress Uncertainty (psi)	Strain Uncertainty
5.975	0.05	8.17E-06	8	0	0	0.00	0.00
5.975	0.68	1.14E-04	114	60.9	668	11.64	10.18
5.975	0.76	1.27E-04	127	121.8	1335	13.48	10.22
5.975	1.34	2.25E-04	225	182.7	2003	16.07	10.68
5.975	1.86	3.11E-04	311	243.6	2670	19.13	11.27
5.975	2.10	3.51E-04	351	304.5	3338	22.45	11.60
5.975	2.69	4.49E-04	449	365.4	4006	25.94	12.51
5.975	3.22	5.39E-04	539	426.3	4673	29.54	13.47
5.975	3.32	5.56E-04	556	487.2	5341	33.21	13.66
5.975	4.17	6.99E-04	699	548.1	6008	36.93	15.39
5.975	4.54	7.60E-04	760	609	6676	40.69	16.18
5.975	4.81	8.05E-04	805	669.9	7343	44.48	16.78
5.975	5.22	8.74E-04	874	730.8	8011	48.29	17.72
5.975	5.74	9.60E-04	960	791.7	8679	52.11	18.93
5.975	6.18	1.03E-03	1034	852.6	9346	55.95	19.98
5.975	6.67	1.12E-03	1115	913.5	10014	59.80	21.18
5.975	6.96	1.16E-03	1165	974.4	10681	63.65	21.91
5.975	6.86	1.15E-03	1148	1035.3	11349	67.52	21.66
5.975	6.98	1.17E-03	1169	1096.2	12017	71.39	21.97

B.5 Extensometer Stress vs. Strain

Time (s)	Elongation (in.)	Force (lb)	Stress (psi)	E (psi)	Strain	Microstrain
0	-6.00E-06	2	23	-3.84E+06	-6.00E-06	-6
0.1	-5.00E-06	2	24	-4.75E+06	-5.00E-06	-5
0.2	1.00E-06	7	73	7.34E+07	1.00E-06	1
0.3	1.00E-05	13	141	1.41E+07	1.00E-05	10
0.4	1.70E-05	19	204	1.20E+07	1.70E-05	17
0.5	2.50E-05	25	270	1.08E+07	2.50E-05	25
0.6	3.20E-05	30	333	1.04E+07	3.20E-05	32
0.7	3.80E-05	35	380	1.00E+07	3.80E-05	38
0.8	4.70E-05	41	450	9.56E+06	4.70E-05	47
0.9	5.10E-05	45	492	9.65E+06	5.10E-05	51
1	6.00E-05	52	567	9.45E+06	6.00E-05	60
1.1	6.50E-05	55	607	9.34E+06	6.50E-05	65
1.2	7.30E-05	61	665	9.12E+06	7.30E-05	73
1.3	7.90E-05	66	727	9.20E+06	7.90E-05	79
1.4	8.50E-05	70	772	9.08E+06	8.50E-05	85
1.5	9.40E-05	77	848	9.02E+06	9.40E-05	94
1.6	9.80E-05	81	885	9.03E+06	9.80E-05	98
1.7	1.06E-04	87	951	8.97E+06	1.06E-04	106
1.8	1.12E-04	92	1004	8.96E+06	1.12E-04	112
1.9	1.19E-04	97	1061	8.92E+06	1.19E-04	119
2	1.28E-04	104	1138	8.89E+06	1.28E-04	128
2.1	1.33E-04	108	1179	8.86E+06	1.33E-04	133
2.2	1.41E-04	114	1255	8.90E+06	1.41E-04	141
2.3	1.48E-04	119	1307	8.83E+06	1.48E-04	148
2.4	1.57E-04	126	1380	8.79E+06	1.57E-04	157
2.5	1.65E-04	132	1450	8.79E+06	1.65E-04	165
2.6	1.70E-04	136	1496	8.80E+06	1.70E-04	170
2.7	1.81E-04	144	1574	8.69E+06	1.81E-04	181
2.8	1.86E-04	148	1624	8.73E+06	1.86E-04	186
2.9	1.97E-04	156	1706	8.66E+06	1.97E-04	197
3	2.04E-04	161	1767	8.66E+06	2.04E-04	204
3.1	2.10E-04	166	1821	8.67E+06	2.10E-04	210
3.2	2.20E-04	173	1900	8.63E+06	2.20E-04	220
3.3	2.27E-04	178	1950	8.59E+06	2.27E-04	227
3.4	2.36E-04	186	2040	8.64E+06	2.36E-04	236
3.5	2.43E-04	190	2087	8.59E+06	2.43E-04	243
3.6	2.50E-04	196	2151	8.61E+06	2.50E-04	250
3.7	2.60E-04	203	2227	8.57E+06	2.60E-04	260
3.8	2.64E-04	208	2278	8.63E+06	2.64E-04	264
3.9	2.75E-04	216	2368	8.61E+06	2.75E-04	275
4	2.83E-04	220	2412	8.52E+06	2.83E-04	283
4.1	2.92E-04	227	2483	8.51E+06	2.92E-04	292
4.2	2.99E-04	233	2554	8.54E+06	2.99E-04	299
4.3	3.05E-04	238	2614	8.57E+06	3.05E-04	305
4.4	3.17E-04	246	2700	8.52E+06	3.17E-04	317
4.5	3.23E-04	250	2743	8.49E+06	3.23E-04	323
4.6	3.31E-04	257	2820	8.52E+06	3.31E-04	331
4.7	3.38E-04	263	2880	8.52E+06	3.38E-04	338
4.8	3.48E-04	269	2952	8.48E+06	3.48E-04	348
4.9	3.57E-04	276	3029	8.49E+06	3.57E-04	357
5	3.63E-04	280	3074	8.47E+06	3.63E-04	363
5.1	3.71E-04	288	3154	8.50E+06	3.71E-04	371
5.2	3.78E-04	293	3210	8.49E+06	3.78E-04	378
5.3	3.88E-04	300	3287	8.47E+06	3.88E-04	388
5.4	3.96E-04	306	3358	8.48E+06	3.96E-04	396
5.5	4.02E-04	311	3408	8.48E+06	4.02E-04	402
5.6	4.12E-04	318	3490	8.47E+06	4.12E-04	412
5.7	4.18E-04	323	3542	8.47E+06	4.18E-04	418
5.8	4.28E-04	331	3627	8.47E+06	4.28E-04	428
5.9	4.35E-04	336	3688	8.48E+06	4.35E-04	435
6	4.43E-04	342	3746	8.46E+06	4.43E-04	443
6.1	4.52E-04	349	3822	8.46E+06	4.52E-04	452
6.2	4.58E-04	353	3872	8.46E+06	4.58E-04	458
6.3	4.69E-04	362	3964	8.45E+06	4.69E-04	469
6.4	4.75E-04	366	4013	8.45E+06	4.75E-04	475
6.5	4.84E-04	372	4078	8.43E+06	4.84E-04	484
6.6	4.91E-04	379	4152	8.46E+06	4.91E-04	491
6.7	5.00E-04	384	4206	8.41E+06	5.00E-04	500
6.8	5.10E-04	392	4299	8.43E+06	5.10E-04	510
6.9	5.14E-04	396	4342	8.45E+06	5.14E-04	514
7	5.24E-04	403	4414	8.42E+06	5.24E-04	524
7.1	5.32E-04	409	4483	8.43E+06	5.32E-04	532
7.2	5.40E-04	415	4545	8.42E+06	5.40E-04	540
7.3	5.51E-04	423	4632	8.41E+06	5.51E-04	551
7.4	5.55E-04	426	4673	8.42E+06	5.55E-04	555
7.5	5.66E-04	434	4752	8.40E+06	5.66E-04	566
7.6	5.71E-04	439	4810	8.42E+06	5.71E-04	571
7.7	5.81E-04	445	4882	8.40E+06	5.81E-04	581
7.8	5.91E-04	452	4957	8.39E+06	5.91E-04	591
7.9	5.95E-04	456	5000	8.40E+06	5.95E-04	595
8	6.05E-04	464	5083	8.40E+06	6.05E-04	605
8.1	6.12E-04	468	5134	8.39E+06	6.12E-04	612